


Nephroprotective Effects of Selenium Nanoparticles Against Sodium Arsenite-Induced Damages

Shubin Li , Xingna Dong, Limeng Xu, Zhenli Wu

Department of Geriatric Medical Center, Inner Mongolia People's Hospital, Hohhot, 010021, People's Republic of China

Correspondence: Zhenli Wu, Email zhenliwu@126.com

Introduction: The potential effects of selenium nanoparticles (SeNPs) administration on arsenic exposure-mediated nephrotoxicity by alleviating fibrosis, inflammation, oxidative stress-related damage, and apoptosis remains more detailed investigations.

Methods: After the synthesis of selenium nanoparticles (SeNPs) by sodium selenite (Na_2SeO_3) through a versatile and green procedure, the biosafety of SeNPs was assessed by assaying renal functions and inflammation in mice. Subsequently, nephroprotective effects of SeNPs against sodium arsenite (NaAsO_2)-induced damages were confirmed by biochemical, molecular, and histopathological assays, including renal function, histological lesion, fibrosis, inflammation, oxidative stress-related damage, and apoptosis in mice renal tissues and renal tubular duct epithelial cells (HK2 cells).

Results: The excellent biocompatibility and safety of SeNPs prepared in this study were confirmed by the non-significant differences in the renal functions and inflammation levels in mice between the negative control (NC) and 1 mg/kg SeNPs groups ($p > 0.05$). The results of biochemical, molecular, and histopathological assays confirmed that daily administration of 1 mg/kg SeNPs for 4 weeks not only ameliorated renal dysfunctions and injuries caused by NaAsO_2 exposure but also inhibited the fibrosis, inflammation, oxidative stress-related damage, and apoptosis in the renal tissues of NaAsO_2 -exposed mice. In addition, altered viability, inflammation, oxidative stress-related damage, and apoptosis in the NaAsO_2 -exposed HK2 cells were effectively reversed after 100 $\mu\text{g/mL}$ SeNPs supplementation.

Conclusion: Our findings authentically confirmed the biosafety and nephroprotective effects of SeNPs against NaAsO_2 exposure-induced damages by alleviating inflammation, oxidative stress-related damage, and apoptosis.

Keywords: selenium nanoparticles, arsenite, nephroprotective, inflammation, oxidative stress, apoptosis

Introduction

Over past decades, accumulating epidemiological studies have confirmed that continuous anthropogenic activities promote the ubiquitous distribution of arsenic in the atmosphere, hydrosphere, lithosphere, biosphere, and anthroposphere.¹ Nearly 108 countries are being affected by arsenic-contaminated groundwater resources and agroecosystems, with concentrations exceeding the World Health Organization (WHO) recommended maximum safe levels (10 $\mu\text{g/L}$ in drinking water or 15 $\mu\text{g/kg}$ inorganic arsenic intake).¹ Seriously, the health of more than 200 million people in Southeast Asian countries, including Bangladesh, China, India, Vietnam, and Thailand, has been compromised by the consumption of arsenic-contaminated groundwater and foods with terrestrial and aquatic origins.¹

As a toxic element belonging to the highest health hazard category, arsenic has already been classified in the Group 1 of carcinogenic compounds known to humans by the International Agency of Research on Cancer (IARC, 2004) and has been described by WHO as “the largest mass poisoning of a population in history”.² In addition, these comprehensive studies have demonstrated that acute or chronic exposure to arsenicals through oral, percutaneous contact, inhalation, or parenteral pathways not only disturbs the expression of genes related to protein translation, signal transduction, transcription regulation, and iron homeostasis but also promote an array of adverse effects through multiple mechanisms including Ca^{2+} homeostasis deregulation, altered reactive oxygen species (ROS) generation, inhibition of DNA repair, mitochondrial dysfunction, and mitochondrial permeability transition (MPT)-dependent apoptosis.²

Regardless of the well-developed mechanism of mammalian bioremediation to resist environmental arsenic,¹ causal relationships between arsenical exposure and altered ROS generation/mitochondrial dysfunctions have been associated with increased risk of breast, skin, bladder, kidney, lung, and liver cancers,³ as well as these various human disorders including neurotoxicity, cardiovascular disease (CVD), diabetes, gastrointestinal disturbances, liver failures, and renal dysfunctions through inducing endoplasmic reticulum (ER)- and oxidative stress-related damages.^{4–7} In laboratory conditions, a recent study from our team initially confirmed oxidative stress-related damage in mammalian gametes caused by arsenic exposure,⁸ consistent with the findings of these substantial publications related to arsenic exposure-induced reproductive toxicities.^{9,10} Most importantly, shreds of evidence also suggest that arsenic exposure is positively associated with alterations in DNA methylation and histone maintenance in mammalian cells, animal models, and humans,¹¹ leading to the transgenerational genotoxicity of arsenic exposure¹² and raising concerns about the effects of arsenic exposure on environmental risk and public health.

In addition, compelling literature has revealed positive corrections between arsenical exposure and nephrotoxicity by promoting oxidative stress-related damage, inflammation, and apoptosis.^{13–15} Moreover, González-Cortés et al confirmed that arsenic exposure disrupted the mammalian extracellular matrix (ECM) remodeling process by altering the expression patterns of genes including *matrix metalloproteinases* (MMPs) and *tissue inhibitors of metalloproteinases* (TIMPs),¹⁶ in turn, resulted in an imbalance between excessive synthesis and reduced ECM component breakdown and triggered progressive renal fibrosis and renal dysfunctions including glomerulosclerosis and end-stage renal diseases.^{17,18}

Over the past decades, natural or synthetic antioxidants such as naringenin,¹⁹ sodium selenite (Na_2SeO_3),^{20,21} betaine,¹⁵ bosentan,¹⁴ tetramethylpyrazine,²² and chlorogenic acid²³ have been used to combat arsenic exposure-induced nephrotoxicity. Encouragingly, these previous publications have confirmed the protective effects of nanotechnology functionalized selenium (Se) nanomedicines including chitosan Se nanoparticles (NPs), porous Se@SiO₂ nanospheres, Se@BSANPs, starch-stabilized SeNPs, Trolox functionalized SeNPs, and lycopene-coated SeNPs against the renal injuries in rats, making the aforementioned Se nanomaterials with excellent antioxidant activity and low toxicity a hotspot.^{24–39} Whereas, the potential effects of SeNPs administration on arsenic exposure-mediated nephrotoxicity by alleviating fibrosis, inflammation, oxidative stress-related damage, and apoptosis has not been reported.

To confirm the hypothesis that SeNPs interventions protect against arsenic exposure-mediated nephrotoxicity by ameliorating fibrosis, inflammation, oxidative stress-related damage, and apoptosis, we fabricated SeNPs using a one-step chemical synthesis routine with nephroprotective effects of SeNPs interventions against in vivo NaAsO_2 exposure-induced renal nephrotoxicity assessed by biochemical, molecular, and histopathological assays including renal function, histological injury, fibrosis, inflammation, oxidative stress-related damage, and apoptosis. In addition, the potential effect of SeNPs supplementation on inflammation, oxidative stress-related damage, and apoptosis of in vitro NaAsO_2 -exposed renal tubular duct epithelial (HK2) cells were analyzed to determine the nephroprotective effect of SeNPs interventions against arsenic exposure-induced nephrotoxicity.

Materials and Methods

Chemicals

Unless otherwise indicated, all chemicals and culture media used in this study were purchased from Sigma-Aldrich (Shanghai, China) and Thermo Fisher (Shanghai, China).

Animals and Ethics Statement

All animal-related experimental protocols applied in this study were conducted according to the standards of the Ethics Committee of Inner Mongolia People's Hospital. Male (5-week-old) C57BL/6 mice, obtained from Beijing SiPeiFu Biotechnology Company, were housed in polyethylene veterinary cages under controlled environmental conditions (temperature: 20–22°C, relative humidity: 60 ± 10% and 12-h light/dark cycles) with a standard balanced rodent diet and water supplied and consumed *ad libitum*.

Synthesis and Characterization of SeNPs

Based on previous literature with small modifications, the synthesis of SeNPs was carried out by a versatile and green method.^{40,41} Briefly, 4 g of sodium selenite (Na_2SeO_3 , S5261, Sigma-Aldrich, Shanghai, China) and 4 g of glucose

(G6172, Macklin, Shanghai, China) were dissolved in 200 mL of 50% ethylene glycol solution (E808737, Macklin, Shanghai, China). After pH was adjusted to 7.2, the reactants were stirred at a constant speed until red signals appeared. The by-product and excess reactants were separated by dialysis for 4 d with a 1000 Da dialysis bag (YA1035, Solarbio, Beijing, China) with the freeze-drying for a subsequent 48 h conducted with a freeze-drying machine to obtain SeNPs. The size and morphology of SeNPs were analyzed by scanning electron microscopy (SEM). In addition, the compositional analysis of SeNPs was performed by an energy dispersive analysis of X-ray spectroscopy (EDAX) microanalysis system coupled with SEM.

Biosafety Assessment of SeNPs

To confirm the *in vivo* biosafety of SeNPs administration, 18 mice were randomly divided into two experimental groups ($n = 9$ per group). For daily drug exposure, the SeNPs administration group was intragastrically administered with 1.0 mg/kg body weight of SeNPs, while the negative control (NC) group was intragastrically administered with the same volume of normal saline.^{23,29} After 14 d of daily drug administration, the plasma of all mice was collected before the mice sacrifice by cervical dislocation. Subsequently, the liver and kidney functions of each group were analyzed by assessing plasma levels of alanine aminotransferase (ALT), aspartate aminotransferase (AST), blood urea nitrogen (BUN), and creatinine (CRE) with an automated chemical analyzer (AU5800, Beckman, Shanghai, China). In addition, plasma inflammation levels in each group were confirmed by assessing plasma levels of IL-1 β and IL-10 with commercial enzyme-linked immunosorbent assay (ELISA) kits (88-7013-88 for IL-1 β and 88-7105-88 for IL-10, Thermo Fisher, Shanghai, China) according to the manufacturer's instructions.

Drug Treatment

After acclimation for 7 d, 25 mice were randomly divided into five experimental groups ($n=5$ per group) as follows: negative control group (NC group, intragastrically administered with normal saline), NaAsO₂ group (intragastrically administered with 5 mg/kg body weight of NaAsO₂), 0.5 mg/kg SeNPs group (intragastrically administered with 5 mg/kg body weight of NaAsO₂ and 0.5 mg/kg body weight of SeNPs), 1 mg/kg SeNPs group (intragastrically administered with 5 mg/kg body weight of NaAsO₂ and 1 mg/kg body weight of SeNPs), and 2 mg/kg SeNPs group (intragastrically administered with 5 mg/kg body weight of NaAsO₂ and 2 mg/kg body weight of SeNPs). The concentration and treatment periods of NaAsO₂ and SeNPs applied in the present study were selected based on these former publications with small modifications.^{23,29} In addition, the mice were intragastrically administered with different concentrations of SeNPs 1 h before the administration of NaAsO₂. According to the experimental design, the mice of each group were daily administered the corresponding drugs for 4 consecutive weeks.

Organ Index Analysis

After drug treatment, the body weight of each mouse was recorded, followed by the collection of plasma and mice sacrifice by cervical dislocation according to the departmental protocols.

After the removal of fat tissues and through washes with phosphate buffer saline (PBS), the wet weight of bilaterally renal tissues in each sacrificed mouse was recorded with the renal index analyzed as the wet weight of renal tissue/body weight $\times 100\%$. After calculating the renal index, renal tissues of each group were dissected into pieces (5 mm \times 5 mm \times 5 mm) by surgical blades, thoroughly washed with PBS solution, and randomly assigned with 30 pieces kept in 10% neutral buffered formalin solution (G2161, Solarbio, Beijing, China) for histological assay, 30 pieces kept in liquid nitrogen for PCR assay, and 30 pieces kept on the freshly prepared ice for tissue homogenization and biochemical analysis.

Renal Function Analysis

To analyze the ameliorative effect of SeNPs interventions against the renal dysfunctions caused by *in vivo* NaAsO₂ exposure, renal function in each group was analyzed with plasma levels of BUN and CRE in each group detected with an automated chemical analyzer.

Histological Staining

Based on the results of renal index and kidney function, the concentrations of SeNPs were optimized for the following experiments. Subsequently, renal tissues from the NC, NaAsO₂, and SeNPs groups were collected, fixed in 10% neutral buffered formalin solution at room temperature for 24 h, and embedded in paraffin. After the preparation of 3 µm sections according to the departmental protocols,⁴² the sections were stained with a commercial hematoxylin and eosin staining (HE) kit (G1120, Solarbio, Beijing, China), a Masson trichrome staining kit (G1345, Solarbio, Beijing, China), or a glycogen periodic acid Schiff (PAS/Hematoxylin) staining kit (G1281, Solarbio, Beijing, China) to confirm the tubular injury, inflammation, and fibrosis levels in each group. Moreover, Van Gieson staining, Resorcinol staining, and Alcian blue staining were applied to confirm the ameliorative effect of SeNPs interventions on the altered ECM remodeling process in the NaAsO₂-exposed renal tissues.⁴³

Immunohistochemistry Staining

To analyze the ameliorative effect of SeNPs interventions on the altered fibrosis, inflammation, and apoptosis in the NaAsO₂-exposed renal tissues, immunohistochemistry (IHC) staining of proteins related to fibrosis (α -SMA and Fibronectin), inflammation (IL-1 β and IL-10), and apoptosis (Bax and Bcl-2) in each group were performed according to the departmental protocols.⁴⁴

Briefly, after dewaxing, gradient rehydration, and antigen retrieval, the paraffin sections of each group were incubated with 10% bovine albumin (BSA, V900933, Sigma-Aldrich, Shanghai, China) at 37 °C for 30 min. The sections after BSA blocking were subsequently incubated with primary antibodies at 4 °C overnight. Detailed information about the primary antibodies used in this study has been supplemented in [Supplementation Table 1](#).

After incubation of primary antibodies, the sections were rinsed three times with PBS solution supplemented with 1% Tween 20 (T8220, Solarbio, Beijing, China) and then incubated with goat anti-rabbit-HRP secondary antibodies (with 1:300 diluted concentrations in PBS solution, ZDR-5306, ZSGB-BIO, Beijing, China) at 25 °C for 2 h. After secondary antibody incubation, the sections were incubated with DAB substrate chromogen solution (DA1010, Solarbio, Beijing, China) at 25 °C for 3 min, followed by counter-staining of hematoxylin solution for 5 min and section sealing with neutral balsam (G8590, Solarbio, Beijing, China). These sealed sections were examined in a blinded fashion under a light microscope (CI-L, Nikon, Tokyo, Japan) with positive IHC staining intensity of each protein in different groups calculated by Image J software.

ELISA

To confirm the ameliorative effect of SeNPs interventions on altered inflammation in NaAsO₂-exposed renal tissues, plasma levels of IL-1 β and IL-10 in each group were analyzed by commercial ELISA kits according to the manufacturer's instructions.

Assays of Antioxidant Potentials

After tissue homogenization, the levels of SOD, GSH, CAT, and MDA in NaAsO₂-exposed renal tissues were analyzed by commercial assay kits (performed in triplicate, S0109 for SOD, S0052 for GSH, BC0205 for CAT, and S0131 for MDA, Beyotime, Shanghai, China) to analyze the ameliorative effect of SeNPs interventions on disturbed antioxidant potentials in the NaAsO₂-exposed renal tissues.

PCR Assay

To analyze the ameliorative effect of SeNPs interventions on the abnormal expression levels of genes related to antioxidant (*Sod2*, *Gpx*, and *Catalase*), fibrosis (α -SMA and *Fibronectin*), inflammation (IL-1 β and IL-10), and apoptosis (*Bax* and *Bcl-2*) in the NaAsO₂-exposed renal tissues, total RNA from each group were extracted by Trizol solution (79,306, Thermo Fisher, Shanghai, China) according to the departmental protocols.⁴³

The reversed syntheses of cDNA were conducted using a commercial Prime ScriptTM RT reagent kit (RR047A, Takara, Dalian, China), followed by real-time PCR analyses within a PikoReal system. Gene expression levels between different groups were calculated using the 2^{- $\Delta\Delta C_t$} method with the ubiquitously expressed *GAPDH* gene used as internal

control.⁴² The primers for reverse transcription PCR and real-time PCR analyses in the current study have been supplemented in [Supplementation Table 2](#).

Cell Culture, Drug Treatment, and Experimental Group Setting

HK2 cells (renal tubular duct epithelial cells), validated by the short tandem repeat (STR) profiling, were purchased from the Cell Bank of Procell Life Science & Technology Company (Wuhan, China) and cultured with the culture medium as Dulbecco's modified eagle medium (DMEM, 11965092, Thermo Fisher, Shanghai, China) supplemented with 10% fetal bovine serum (FBS, 10099141C, Thermo Fisher, Shanghai, China) and 100 IU/mL penicillin/streptomycin antibiotics (P/S, 15070063, Thermo Fisher, Shanghai, China) in a CO₂ incubator (37.0 °C, 5% CO₂).

For in vitro exposure to NaAsO₂, 5 ng/mL NaAsO₂ was dissolved in the culture medium with the experimental group set as NaAsO₂ group.⁴⁵ In addition, NaAsO₂-exposed HK2 cells were supplemented with 50, 100, and 200 µg/mL SeNPs solution.⁴⁶ Moreover, HK2 cells treated with a basic culture medium, instead of NaAsO₂ or SeNPs exposure, were set as the normal control group (NC group). After drug treatment in a CO₂ incubator (37.0 °C, 5% CO₂) for 24 h, HK2 cells from each group were collected for the following assays.

Viability Assay

According to the departmental protocols, an MTT assay was applied to confirm the potential effect of SeNPs supplementation on the viability deficiency of renal cells induced by in vitro NaAsO₂ exposure and optimize the SeNPs concentration applied for the following assay.

After drug treatment, 10 µL MTT reagents (5 mg/mL, C0009S, Beyotime, Shanghai, China) were added to the culture medium of different groups with culture plates incubated at 37 °C for another 4 h. After the addition of 100 µL dimethyl sulfoxide (DMSO, CD4731, Coolaber, Beijing, China) solution and subsequent incubation at 37 °C for 3 h, the absorbance at 570 nm of culture plates was measured by a microplate reader with the optimization of SeNPs concentration further analyzed.

Assays of Cellular Inflammation Level

After drug treatment, the potential effect of SeNPs supplementation against inflammation in renal cells induced by in vitro NaAsO₂ exposure was analyzed by ELISA with the supernatant levels of IL-1β and IL-10 in each group analyzed according to the manufacturer's instructions.

Mitochondrial Function Analysis

According to the departmental protocols, the effect of SeNPs supplementation on mitochondrial dysfunctions in renal cells induced by in vitro NaAsO₂ exposure was analyzed by assessing mitochondrial activity and Mitochondrial Membrane Potentials (ΔΨ_m) of renal cells by MitoTracker staining and JC-1 staining.⁸

For MitoTracker staining, HK2 cells after drug treatments were thoroughly washed with Dulbecco's phosphate buffered saline solution (DPBS, 14190250, Thermo Fisher Scientific, Beijing, China) and incubated with 4% paraformaldehyde solution (PFA, P1110, Solarbio, Beijing, China) at room temperature for 15 min. Subsequently, HK2 cells from each group were incubated with 200 nM MitoTracker staining solution (C1049, Beyotime, Shanghai, China) at 37 °C for 30 min. After incubation of 10 µg/mL DAPI staining solution (C0065, Solarbio, Beijing, China), the MitoTracker staining density of each group was analyzed by Image J software.

For JC-1 staining, HK2 cells after PFA fixation were incubated with 10 µM JC-1 staining solution (C2006, Beyotime, Shanghai, Zhejiang, China) at 37 °C for 20 min, followed by further incubation of DAPI staining solution and subsequent analysis of staining intensity by Image J software.

ROS Generation Assay

To analyze the ameliorative effect of SeNPs supplementation on antioxidant abnormality of renal cells caused by in vitro NaAsO₂ exposure, ROS generation level of HK2 cells was detected with a ROS generation assay kit (S0033, Beyotime, Shanghai, China) according to the manufacturer's instructions.⁸

Briefly, HK2 cells after drug treatments were incubated with 10 μ M dichlorofluorescein diacetate solution (DCFH-DA) at 37 °C for 30 min and re-incubated with DAPI staining solution with the ROS generation level of each group observed under a confocal microscope and quantification of DCFH-DA staining intensity in each group conducted by Image J software.

Assays of Cellular Antioxidant Potentials

To further confirm the potential effect of SeNPs supplementation on altered antioxidant potentials of renal cells induced by in vitro NaAsO₂ exposure, the levels of SOD, GSH, CAT, and MDA of each group were analyzed by commercial assay kits according to the manufacturer's instructions.

Assays of Cellular Apoptosis

To analyze the potential effect of SeNPs supplementation on apoptosis of renal cells induced by in vitro NaAsO₂ exposure, expression of apoptosis-related proteins (γ H2A) in HK2 cells was analyzed by immunofluorescence (IF) staining.⁸

Briefly, HK2 cells from each group were washed three times with DPBS solution containing 1% Tween 20 solution and fixed with 4% PFA at 37 °C for 30 min. Subsequently, HK2 cells were permeabilized with 0.5% Triton X-100 solution (T8200, Solarbio, Beijing, China) at 37 °C for 30 min and incubated with 5% BSA solution (SW3015, Solarbio, Beijing, China) at 37 °C for 30 min. HK2 cells were then incubated with primary antibody at 4 °C overnight. Detailed information about γ H2A antibody has been supplemented in [Supplementation Table 1](#).

After incubation of Alexa Fluor[®] 555 secondary antibody (with 1:300 dilutions in DPBS solution, ab150074, Abcam, Shanghai, China) for 1 h, HK2 cells from each group were incubated with the DAPI staining solution, mounted on glass slides, and examined under a confocal microscope with the γ H2A staining intensity of each group calculated by Image J software.

Statistical Analysis

Analyses of experimental data in this study were carried out with the Statistical Package for the Social Sciences (SPSS, IBM, Version 19.0). All descriptive statistics were presented as mean \pm standard deviation (SD) and assessed by parametric (one-way ANOVA LSD test) and nonparametric (Wilcoxon) tests, based on the results of residual normality (Gaussian distribution) and variance homogeneity. Differences were considered significant at $p < 0.05$.

Results

Characterization and Biocompatibility of SeNPs

As shown in [Figure 1A](#), TEM images of SeNPs and micrograph assays confirmed the spherical structure of SeNPs with a diameter of 40–60 nm ([Figure 1B](#)). XRD pattern of SeNPs showed a broad peak at about $2\theta = 22^\circ$ ([Figure 1C](#)). There were no sharp and narrow diffraction peaks in the XRD spectra of SeNPs. In addition, the XRD peak shape results suggested the same amorphous structure of SeNPs compared to previous studies.^{47,48}

When compared with the NC group, non-significant changes in plasma parameters including BUN, CRE, ALT, and AST were found in the SeNPs administration group ([Figure 1D–G](#), $p > 0.05$). Evidenced by these non-significant differences in the plasma parameters including IL-1 β ([Figure 1H](#)) and IL-10 ([Figure 1I](#)) between the SeNPs and NC groups ($p > 0.05$), the above results, notably demonstrated the excellent biocompatibility and safe nature of SeNPs prepared in this study.

Effect of SeNPs Interventions on Renal Dysfunctions Caused by the in vivo NaAsO₂ Exposure

During the study period, no treatment-related mortality was observed in animals treated with NaAsO₂ and/or SeNPs. In addition, there were no significant differences in renal index between the NC, NaAsO₂, and SeNPs groups ([Figure 2A](#), $p > 0.05$).

In contrast, significant increments in plasma BUN and CRE levels in NaAsO₂-exposed mice were observed as compared to the NC group ([Figure 2B and C](#), $p < 0.05$), confirming the adverse effect of in vivo NaAsO₂ exposure on mice renal function. Whereas, SeNPs interventions effectively attenuated NaAsO₂ exposure-induced renal dysfunctions,

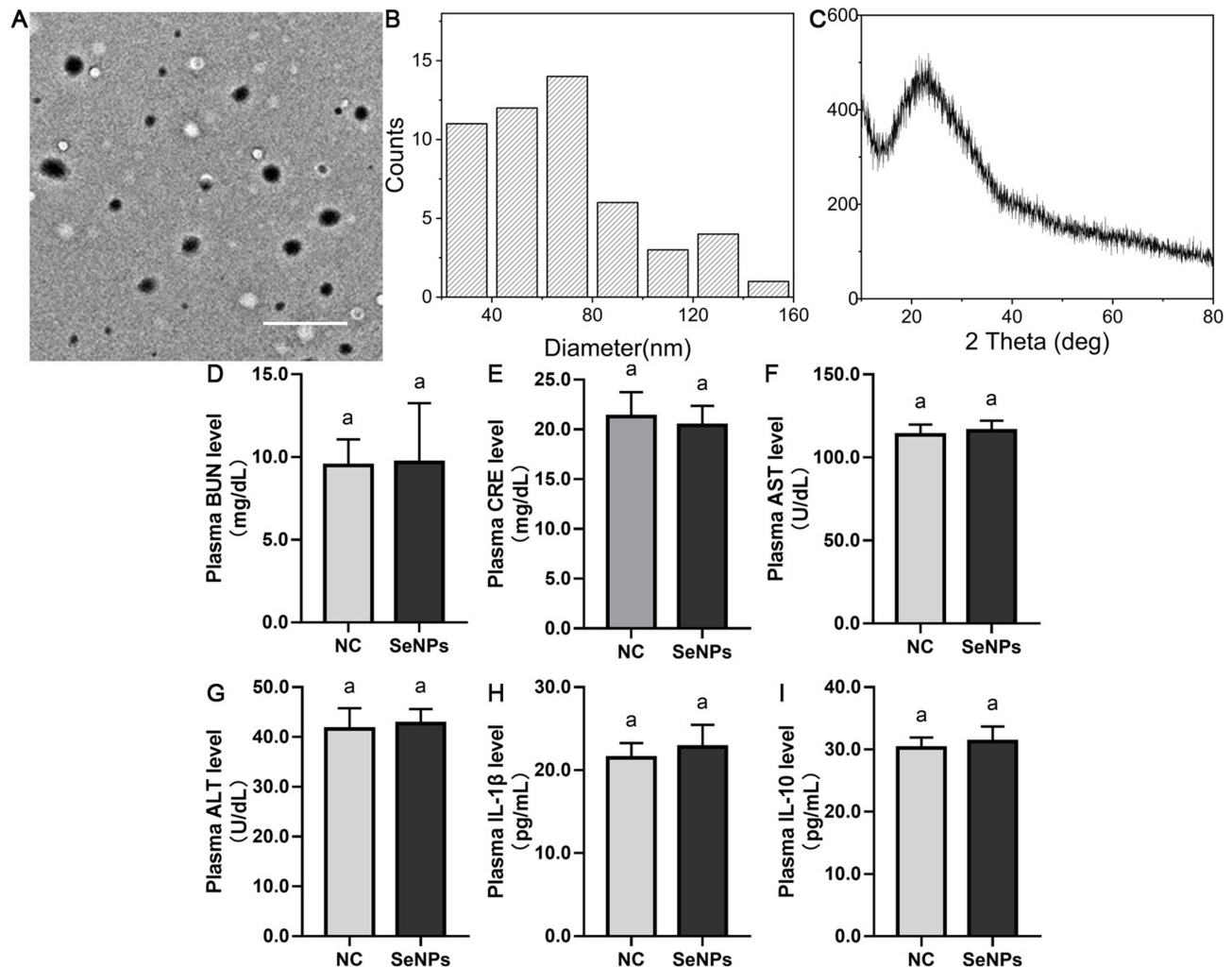


Figure 1 Characterization and biocompatibility of SeNPs. (A) TEM assessment of SeNPs. (B) Particles size distribution of SeNPs. (C) XRD pattern of SeNPs. (D) Plasma BUN level. (E) Plasma CRE level. (F) Plasma AST level. (G) Plasma ALT level. (H) Plasma IL-1 β level. (I) Plasma IL-10 level.

Notes: (A) Scale bar= 1 μ m. (D–I) NC and SeNPs represent negative control and SeNPs administration groups. The same lowercase letter (a) labeled in each column indicates non-significant differences between the NC and SeNPs groups ($p>0.05$).

as evidenced by the significantly lower plasma levels of BUN and CRE in all SeNPs intervention groups compared to those in the NaAsO₂ group ($p<0.05$, Figure 2B and C). Due to the non-significant differences in plasma BUN and CRE levels between the 1 mg/kg and 2 mg/kg SeNPs intervention groups ($p>0.05$, Figure 2B and C), the 1 mg/kg SeNPs intervention group was selected for the following experiments.

Effect of SeNPs Interventions on Abnormal Renal Fibrosis Caused by in vivo NaAsO₂ Exposure

As indicated in Figure 3A, the results of HE staining confirmed pathological injuries including glomerular hypertrophy, thickening of the tubular basement membrane, deterioration of the renal tubular structure, and peritubular inflammation in the mice renal tissues due to in vivo NaAsO₂ exposure, consistent with these previous studies.^{23,49}

Meanwhile, the results of PAS staining (Figure 3B) and Masson trichrome staining (Figure 3C) confirmed renal fibrosis and collagen disposition in NaAsO₂-exposed renal tissues. In contrast, the alleviating effect of SeNPs

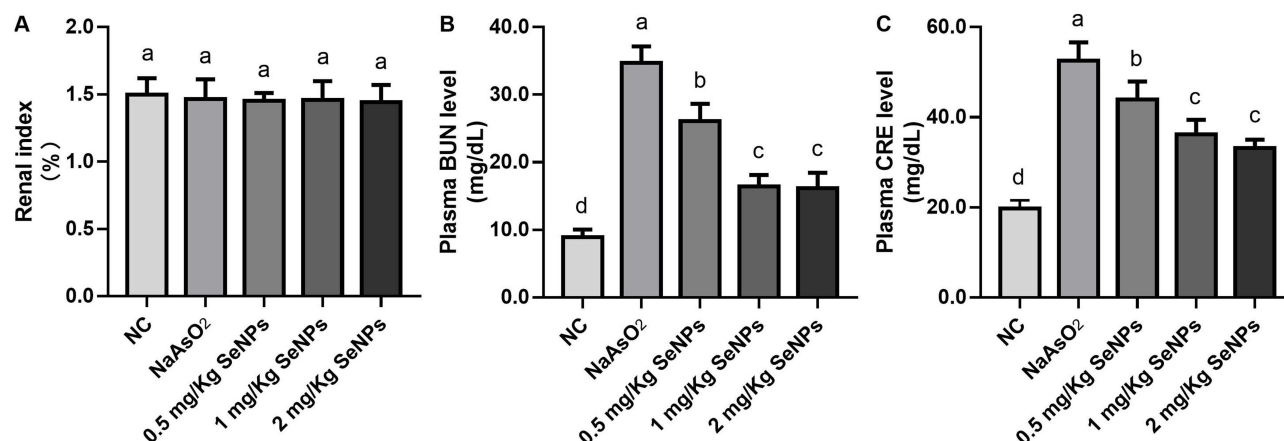


Figure 2 Effect of SeNPs interventions on renal dysfunctions caused by in vivo NaAsO₂ exposure. (A) Renal index. (B) Plasma BUN level. (C) Plasma CRE level.

Notes: (A) NC, NaAsO₂, 0.5 mg/kg SeNPs, 1 mg/kg SeNPs, and 2 mg/kg SeNPs represent negative control, 10 mg/kg NaAsO₂ exposure, 10 mg/kg NaAsO₂ supplemented with 0.5 mg/kg SeNPs, 10 mg/kg NaAsO₂ supplemented with 1 mg/kg SeNPs, and 10 mg/kg NaAsO₂ supplemented with 2 mg/kg SeNPs groups. The same lowercase letter (a) labeled in each column indicates non-significant differences between the corresponding experimental groups ($p > 0.05$). (B and C) NC, NaAsO₂, 0.5 mg/kg SeNPs, 1 mg/kg SeNPs, and 2 mg/kg SeNPs represent negative control, 10 mg/kg NaAsO₂ exposure, 10 mg/kg NaAsO₂ supplemented with 0.5 mg/kg SeNPs, 10 mg/kg NaAsO₂ supplemented with 1 mg/kg SeNPs, and 10 mg/kg NaAsO₂ supplemented with 2 mg/kg SeNPs groups. Different lowercase letters (a, b, c, etc.) labeled in each column indicate significant differences between the corresponding experimental groups ($p < 0.05$).

interventions on halting pathological damage and fibrosis in NaAsO₂-exposed renal tissues were effectively confirmed by the observation of reductions in tubular alternation and collagen disposition in the SeNPs intervention group (Figure 3A–C).

Compared to the NC group, the cumulative distribution of glycosaminoglycan in the NaAsO₂ group was confirmed by the assessment of alcian blue staining (Figure 3D). At the same time, altered glycosaminoglycan level in NaAsO₂-exposed renal tissues was effectively ameliorated by the SeNPs interventions. Consistent with that of the Masson trichrome staining, the result of Resorcinol staining, shown in Figure 3E, revealed interstitial fibrosis caused by in vivo NaAsO₂ exposure through the promotion of elastin accumulation in renal interstitium. In contrast, altered elastin accumulation in the NaAsO₂-exposed renal tissues was effectively inhibited by the SeNPs intervention. In the collagen assay, the result of Van Gieson staining (Figure 3F) confirmed that in vivo NaAsO₂ exposure significantly altered renal collagen distribution. However, SeNPs interventions effectively ameliorated the renal collagen distribution caused by in vivo NaAsO₂ exposure, confirming the beneficial effect of SeNPs interventions on renal fibrosis caused by in vivo NaAsO₂ exposure.

The gene and protein expression levels of α -SMA (Figure 3G, I and K) and fibronectin (Figure 3H, J and L) in the NaAsO₂ group were notably higher than those in the NC group ($p < 0.05$), demonstrating the effect of in vivo NaAsO₂ exposure on inducing renal fibrosis. Effective decreases in gene and protein expression levels of α -SMA and fibronectin from the NaAsO₂ group to the SeNPs group were found (Figure 3G–L, $p < 0.05$), revealing the recuperative effect of SeNPs interventions against fibrosis in NaAsO₂-exposed renal tissues.

Effect of SeNPs Interventions on the Increased Oxidative Stress-Related Damage Caused by the in vivo NaAsO₂ Exposure

Consistent with our former study,⁸ previous publications have confirmed that arsenic exposures trigger carcinogenicity, hepatotoxicity, neurotoxicity, and reproductivity via promoting oxidative stress-related damage.^{50,51} To confirm the potential effect of SeNPs interventions on ameliorating oxidative stress-related damage caused by in vivo NaAsO₂ exposure, antioxidant potentials of each group were analyzed by assessing SOD, GSH, CAT, and MDA levels in mice renal tissues. Meanwhile, qRT-PCR of genes related to the regulation of the mammalian antioxidant defense system was also conducted.

The results revealed that renal SOD (Figure 4A), GSH (Figure 4B), and CAT (Figure 4C) activities in NaAsO₂-exposed renal tissues were significantly lower than those in the NC group ($p < 0.05$), whereas MDA activity (Figure 4D) in the NaAsO₂ group was significantly up-regulated compared to the NC group ($p < 0.05$). Combined with significantly

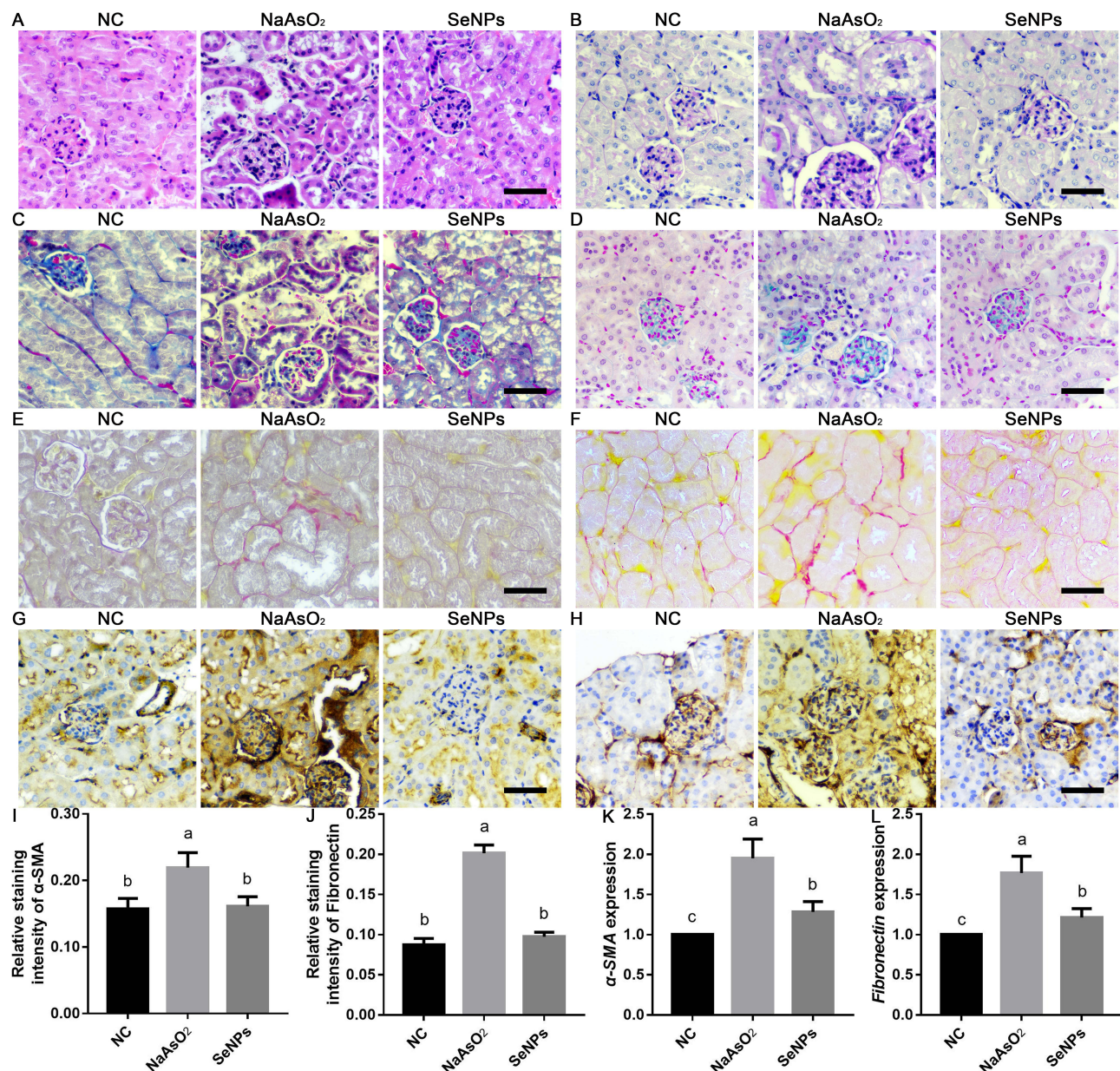


Figure 3 Effect of SeNPs interventions on abnormal renal fibrosis caused by in vivo NaAsO₂ exposure. (A) HE staining. (B) PAS staining. (C) Masson trichrome staining. (D) Alcian blue staining. (E) Resorcinol staining. (F) Van Gieson staining. (G) IHC staining of α-SMA. (H) IHC staining of fibronectin. (I) Relative staining intensity of α-SMA. (J) Relative staining intensity of fibronectin. (K) α-SMA expression. (L) Fibronectin expression.

Notes: (A–G) NC, NaAsO₂, and SeNPs represent negative control, NaAsO₂ exposure, and NaAsO₂ supplemented with SeNPs groups. Scale=50 μm. (H) NC, NaAsO₂, and SeNPs represent the negative control, NaAsO₂ exposure, and NaAsO₂ supplemented with SeNPs groups. Scale=50 μm. (I and J) NC, NaAsO₂, and SeNPs represent the negative control, NaAsO₂ exposure, and NaAsO₂ supplemented with SeNPs groups. Scale=50 μm. (K and L) NC, NaAsO₂, and SeNPs represent negative control, NaAsO₂ exposure, and NaAsO₂ supplemented with SeNPs groups. Different lowercase letters (a, b, c, etc.) labeled in each column of each panel indicate significant differences between the corresponding experimental groups (p<0.05).

lower expression levels of *Sod2*, *Gpx*, and *Catalase* in the NaAsO₂ group compared with those in the NC group (Figure 4E–G, p<0.05), these results confirmed the effect of NaAsO₂ exposure on triggering oxidative stress-related damage in mice renal tissues.

We found that the renal SOD, GSH, and CAT activities in the SeNPs group were effectively up-regulated compared to the NaAsO₂ group (p<0.05). In terms of the renal MDA activity assay, the results showed that SeNPs interventions effectively inhibited the altered renal MDA activity due to NaAsO₂ exposure (p<0.05). Along with remarkably elevated expression levels of *Sod2*, *Gpx*, and *Catalase* in the SeNPs group compared to those in the NaAsO₂ group (p<0.05), these

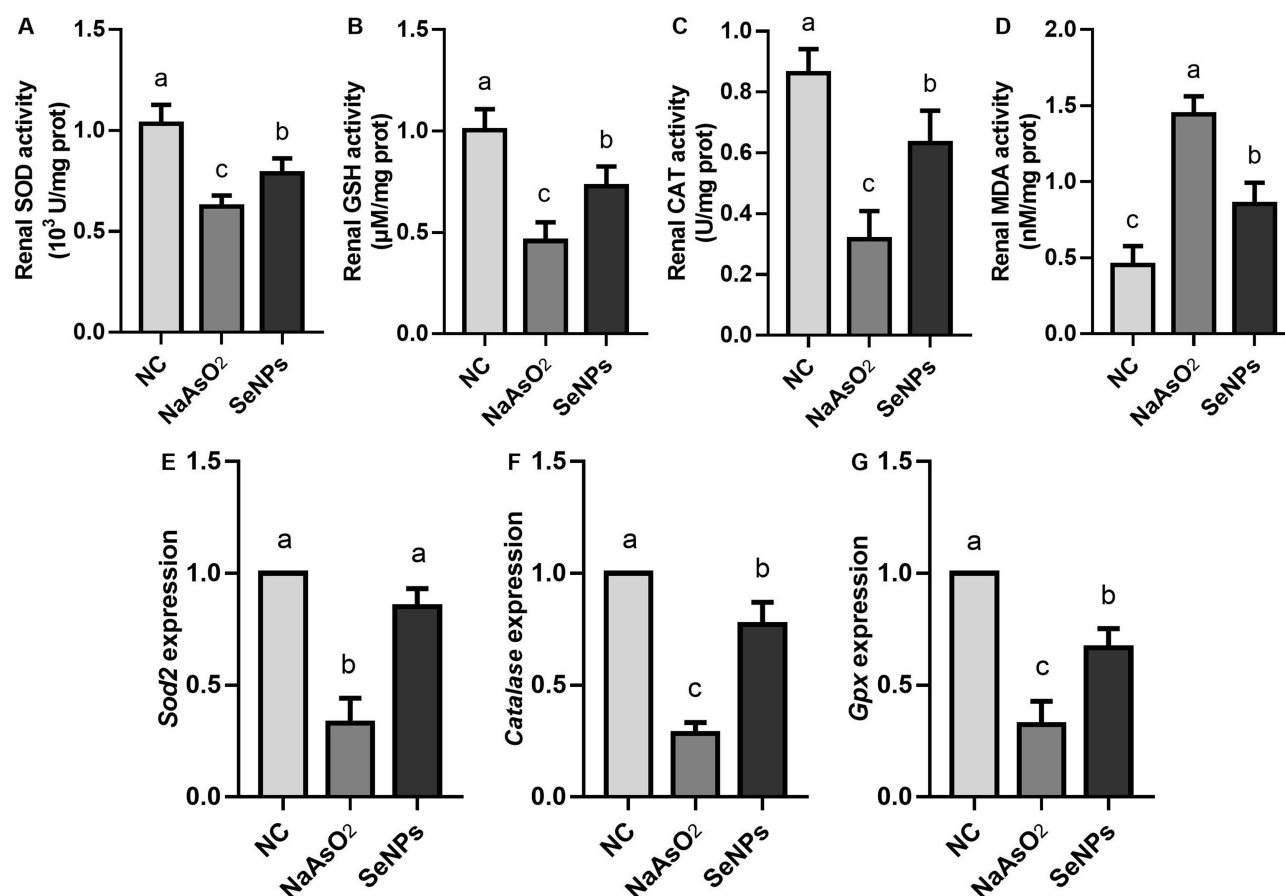


Figure 4 Effect of SeNPs interventions on increased oxidative stress-related damage caused by in vivo NaAsO₂ exposure. **(A)** Renal SOD activity. **(B)** Renal GSH activity. **(C)** Renal CAT activity. **(D)** Renal MDA activity. **(E)** *Sod2* expression. **(F)** *Catalase* expression. **(G)** *Gpx* expression.

Notes: **(A, B and D)** NC, NaAsO₂, and SeNPs represent negative control, NaAsO₂ exposure, and NaAsO₂ supplemented with SeNPs groups. Different lowercase letters (a, b, c, etc.) labeled in each column indicate significant differences between the corresponding experimental groups ($p < 0.05$). **(C)** NC, NaAsO₂, and SeNPs represent negative control, NaAsO₂ exposure, and NaAsO₂ supplemented with SeNPs groups. Different lowercase letters (a, b, c, etc.) in each column indicate significant differences between the corresponding experimental groups ($p < 0.05$). **(E–G)** NC, NaAsO₂, and SeNPs represent negative control, NaAsO₂ exposure, and NaAsO₂ supplemented with SeNPs groups. Different lowercase letters (a, b, c, etc.) labeled in each column of each panel indicate significant differences between the corresponding experimental groups ($p < 0.05$).

noteworthy results suggested the promising effect of SeNPs interventions on attenuating oxidative stress-related damage induced by in vivo NaAsO₂ exposure.

Effect of SeNPs Interventions on Abnormal Renal Inflammation and Altered Apoptosis Caused by the in vivo NaAsO₂ Exposure

Inflammation levels in each group were analyzed by IHC staining, qRT-PCR, and ELISA of IL-1 β and IL-10 in mice plasma and renal tissues to confirm whether SeNPs interventions could protect against NaAsO₂ exposure-induced renal inflammation.

As shown in Figure 5, the results of ELISA and IHC staining confirmed that in vivo NaAsO₂ exposure not only promoted the expression level of IL-1 β in mice renal tissues and release of IL-1 β into plasma (Figure 5A, C and D) but also severely inhibited the expression level of IL-10 in mice renal tissues and release of IL-10 into plasma (Figure 5B, E and F), which was consistent with the gene expression patterns of *IL-1 β* and *IL-10* between the NC and NaAsO₂ groups (Figure 5K and L, $p < 0.05$).

In contrast, the expression patterns of IL-1 β and IL-10 in mice plasma and renal tissues after the SeNPs interventions confirmed the negative corrections between SeNPs interventions and NaAsO₂ exposure-induced renal inflammation, as evidenced by the different protein and gene expression patterns of IL-1 β and IL-10 between the SeNPs and NaAsO₂ groups ($p < 0.05$). In addition, protein and gene expression levels of IL-1 β in mice renal tissues after SeNPs intervention

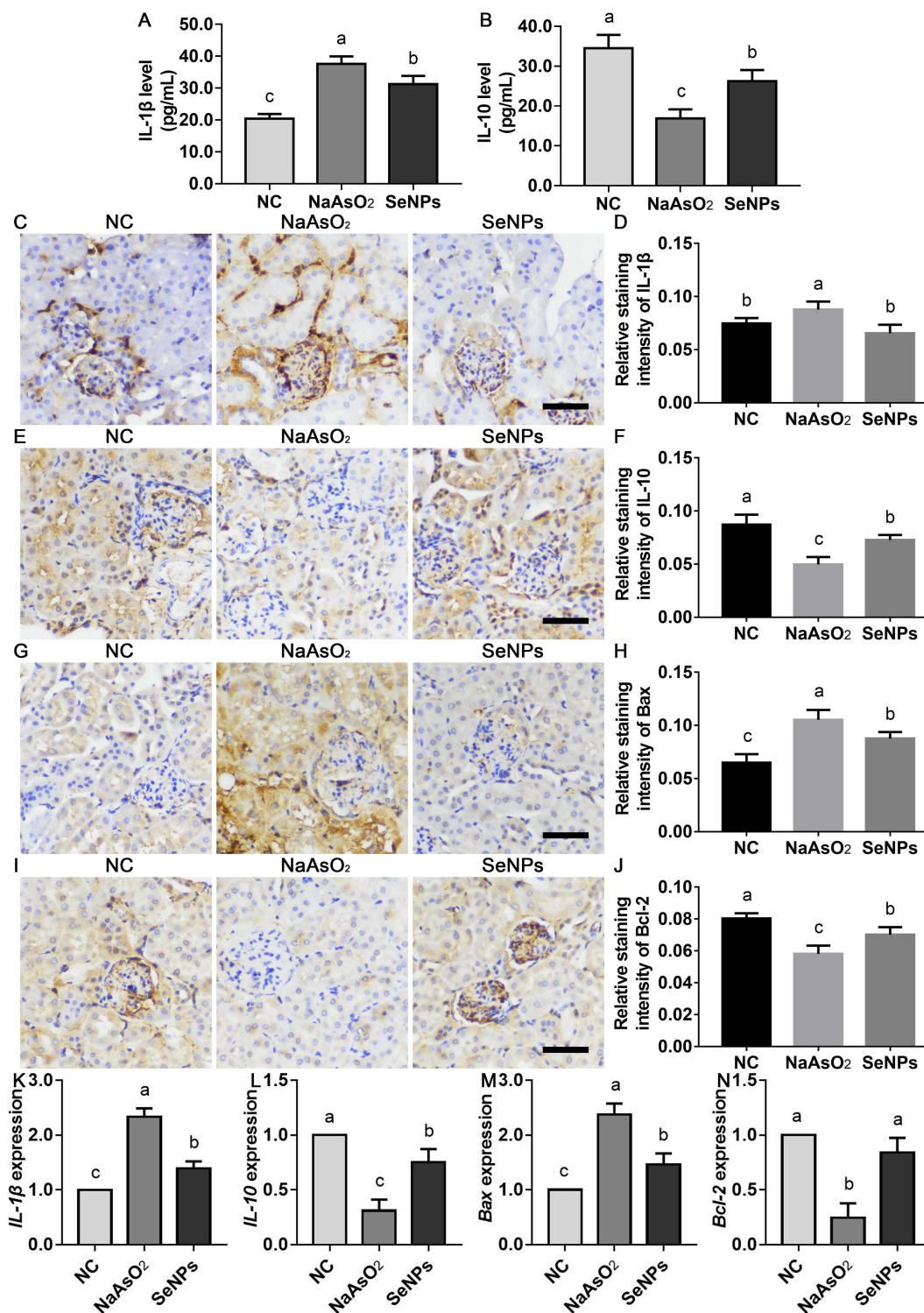


Figure 5 Effect of SeNPs interventions on abnormal renal inflammation and altered apoptosis caused by the in vivo NaAsO₂ exposure. **(A)** Plasma IL-1 β levels. **(B)** Plasma IL-10 levels. **(C)** IHC staining of IL-1 β . **(D)** Relative staining intensity of IL-1 β . **(E)** IHC staining of IL-10. **(F)** Relative staining intensity of IL-10. **(G)** IHC staining of Bax. **(H)** Relative staining intensity of Bax. **(I)** IHC staining of Bcl-2. **(J)** Relative staining intensity of Bcl-2. **(K)** IL-1 β expression. **(L)** IL-10 expression. **(M)** Bax expression. **(N)** Bcl-2 expression. **Notes:** **(A)** NC, NaAsO₂, and SeNPs represent negative control, NaAsO₂ exposure, and NaAsO₂ supplemented with SeNPs groups. Different lowercase letters (a, b, c, etc.) in each column indicate significant differences between the corresponding experimental groups ($p < 0.05$). **(B, D, F, H and J)** NC, NaAsO₂, and SeNPs represent negative control, NaAsO₂ exposure, and NaAsO₂ supplemented with SeNPs groups. Different lowercase letters (a, b, c, etc.) labeled in each column indicate significant differences between the corresponding experimental groups ($p < 0.05$). **(C, E, G and I)** NC, NaAsO₂, and SeNPs represent negative control, NaAsO₂ exposure, and NaAsO₂ supplemented with SeNPs groups. Scale=50 μ m. **(K–M)** NC, NaAsO₂, and SeNPs represent negative control, NaAsO₂ exposure, and NaAsO₂ supplemented with SeNPs groups. Different lowercase letters (a, b, c, etc.) labeled in each column of each panel indicate significant differences between the corresponding experimental groups ($p < 0.05$).

were effectively suppressed, consistent with ELISA results. Compared with those in the NaAsO₂ group, the remarkably up-regulated IL-10 expression level in the SeNPs group ($p < 0.05$) promisingly revealed the beneficial effect of SeNPs interventions against renal inflammation caused by the in vivo NaAsO₂ exposure.

As shown in Figure 5, we found that the Bax staining intensity in the NaAsO₂ group was significantly higher than that in the NC group (Figure 5G and H, $p < 0.05$), whereas the Bcl-2 staining intensity in the NaAsO₂ group was significantly lower than that in the NC group (Figure 5I and J, $p < 0.05$), confirming the adverse effect of NaAsO₂ exposure on exacerbating the renal development through upstreaming cellular apoptosis.^{23,52} We also found that SeNPs interventions not only inhibited Bax staining intensity (Figure 5G and H, $p < 0.05$) but also remarkably promoted Bcl-2 staining intensity in NaAsO₂-exposed mice renal tissues (Figure 5I and J, $p < 0.05$). Combined with the expression patterns of *Bax* and *Bcl-2* (Figure 5M and N), indicating apoptosis in mice renal tissues, the above results provided a pleasant condition that SeNPs interventions could efficaciously avert renal inflammation and apoptosis caused by the in vivo NaAsO₂ exposure.

Effect of SeNPs Supplementation on Fibrosis, Oxidative Stress-Related Damage, Inflammation, and Apoptosis in NaAsO₂-Exposed HK2 Cells

Compared to the NC group, the viability of HK2 cells exposed to NaAsO₂ was significantly reduced (Supplementation Figure 1, $p < 0.05$), confirming NaAsO₂-induced cytotoxicity in HK2 cells.²² In contrast, SeNPs supplementation effectively ameliorated the decreased viability of NaAsO₂-exposed HK2 cells, as demonstrated by the remarkably increased viability of SeNPs supplementation groups (Supplementation Figure 1, $p < 0.05$). Based on the MTT result, 100 µg/mL SeNPs supplementation was selected for the following assay due to the non-significant difference existing in viability between the 100 and 200 µg/mL SeNPs supplementation groups ($p > 0.05$).

As for the effect assessment of SeNPs supplementation on mitochondrial dysfunctions in NaAsO₂-exposed HK2 cells, the severe decrease in MitoTracker staining intensity (Figure 6A and B, $p < 0.05$) and $\Delta\Psi_m$ potentials (relative J-AGG/J-MON ratio, Figure 6C and D, $p < 0.05$) from the NC group to the NaAsO₂ group confirmed mitochondrial dysfunctions in NaAsO₂-exposed HK2 cells. In contrast, SeNPs supplementation not only ameliorated the reduced staining intensity of MitoTracker in HK2 cells caused by NaAsO₂ exposure ($p < 0.05$) but also inhibited altered $\Delta\Psi_m$ potentials of the NaAsO₂-exposed HK2 cells ($p < 0.05$), confirming the beneficial effect of SeNPs supplementation on the mitochondrial functions of NaAsO₂-exposed HK2 cells.

As shown in Figure 6E and F, we also found that DCFH-DA staining intensity in the NaAsO₂ group was seriously increased compared to that in the NC group ($p < 0.05$), confirming that NaAsO₂ exposure promoted ROS generation in HK2 cells. Whereas, altered ROS generation level in NaAsO₂-exposed HK2 cells was efficaciously attenuated after SeNPs supplementation, as evidenced by a significant difference in DCFH-DA staining intensity between the NaAsO₂ and SeNPs groups ($p < 0.05$).

In addition, SOD, GSH, and CAT activities in the NaAsO₂-exposed HK2 cells were seriously reduced compared to those in the NC group (Figure 6G–I, $p < 0.05$), consistent with the above in vivo results. Combined with elevated MDA activity in the NaAsO₂ group compared to the NC group (Figure 6J, $p < 0.05$), these biochemical content assays confirmed the potential effect of NaAsO₂ exposure on triggering oxidative stress-related damage in HK2 cells. After SeNPs supplementation, SOD, GSH, and CAT activities in HK2 cells were effectively increased compared to those in the NaAsO₂ group ($p < 0.05$). Regardless of the significant differences found in SOD, GSH, and CAT activities between the SeNPs and NC groups ($p < 0.05$), the decreased MDA activity in the SeNPs group compared to that in the NaAsO₂ group ($p < 0.05$) at least confirmed the ameliorative effects of SeNPs supplementation on attenuating oxidative stress-related damage induced by NaAsO₂ exposure.

For inflammation evaluations, the ELISA results, shown in Figure 6K and L, confirmed that NaAsO₂ exposure not only remarkably promoted IL-1 β level in HK2 cells ($p < 0.05$) but effectively inhibited IL-10 level in HK2 cells ($p < 0.05$). After SeNPs supplementation, altered expression levels of IL-1 β and IL-10 levels in NaAsO₂-exposed HK2 cells were effectively ameliorated.

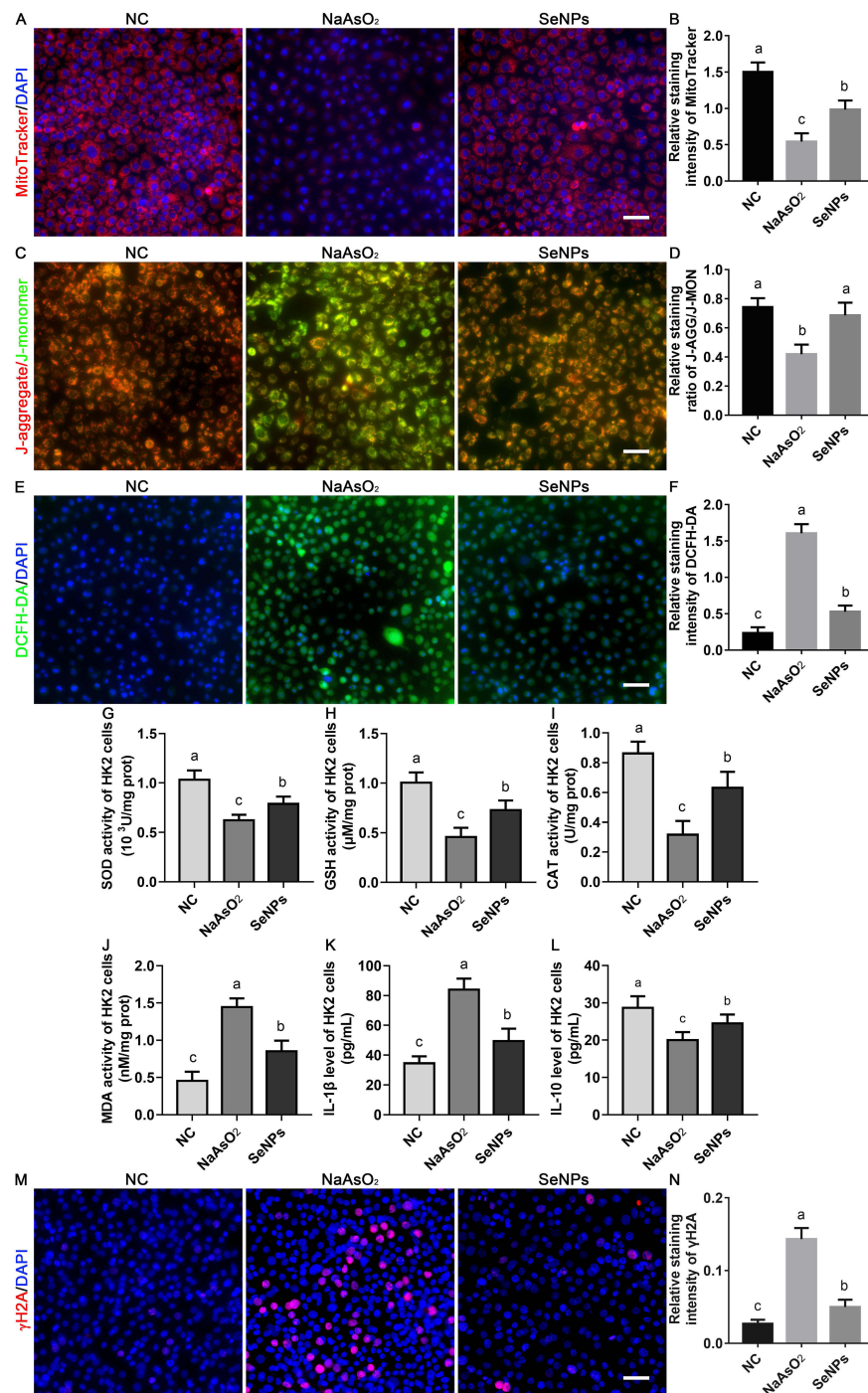


Figure 6 Effect of SeNPs supplementation on inflammation, oxidative stress-related damage, and apoptosis in NaAsO₂-exposed HK2 cells. **(A)** Representative MitoTracker staining result. **(B)** Relative staining intensity of MitoTracker. **(C)** Representative J-C-I staining result. **(D)** Relative staining ratio of J-AGG/J-MON. **(E)** Representative DCFH-DA staining result. **(F)** Relative staining intensity of DCFH-DA. **(G)** SOD activity of HK2 cells. **(H)** GSH activity of HK2 cells. **(I)** CAT activity of HK2 cells. **(J)** MDA activity of HK2 cells. **(K)** IL-1 β level of HK2 cells. **(L)** IL-10 level of HK2 cells. **(M)** Representative IF staining results of γ H2A. **(N)** Relative staining intensity of γ H2A.

Notes: **(A)** NC, NaAsO₂, and SeNPs represent negative control, NaAsO₂ exposure, and NaAsO₂ supplemented with SeNPs groups. MitoTracker represents MitoTracker staining specific for mitochondrial activity. DAPI represents DAPI staining. Scale bar=50 μ m. **(B, F–L and M)** NC, NaAsO₂, and SeNPs represent negative control, NaAsO₂ exposure, and NaAsO₂ supplemented with SeNPs groups. Different lowercase letters (a, b, c, etc.) labeled in each column indicate significant differences between the corresponding experimental groups ($p < 0.05$). **(C)** NC, NaAsO₂, and SeNPs represent negative control, NaAsO₂ exposure, and NaAsO₂ supplemented with SeNPs groups. Different lowercase letters (a, b, c, etc.) labeled in each column indicate significant differences between the corresponding experimental groups ($p < 0.05$). **(D)** NC, NaAsO₂, and SeNPs represent negative control, NaAsO₂ exposure, and NaAsO₂ supplemented with SeNPs groups. Different lowercase letters (a, b, c, etc.) labeled in each column indicate significant differences between the corresponding experimental groups ($p < 0.05$). **(E)** NC, NaAsO₂, and SeNPs represent negative control, NaAsO₂ exposure, and NaAsO₂ supplemented with SeNPs groups. Different lowercase letters (a, b, c, etc.) labeled in each column indicate significant differences between the corresponding experimental groups ($p < 0.05$). **(M)** NC, NaAsO₂, and SeNPs represent negative control, NaAsO₂ exposure, and NaAsO₂ supplemented with SeNPs groups. Different lowercase letters (a, b, c, etc.) labeled in each column indicate significant differences between the corresponding experimental groups ($p < 0.05$).

Finally, the results of the apoptosis assay showed that the IF staining intensity of γ H2A (Figure 6M and N) in HK2 cells was significantly increased after NaAsO₂ exposure as compared with that in the NC group ($p < 0.05$), suggesting the detrimental effect of NaAsO₂ exposure on the apoptosis of HK2 cells. In contrast, a reduction in the positive staining signals of γ H2A was observed in the SeNPs group compared to that in the NaAsO₂ group ($p < 0.05$), which was highly indicative of the nephroprotective effect of SeNPs supplementation against the cytotoxicity of NaAsO₂ exposure via alleviating the NaAsO₂ exposure-induced inflammation, oxidative stress-related damage, and apoptosis.

Discussion

Decades of previous literature have highlighted the nephrotoxicity caused by overdosed exposures to a variety of nephrotoxins, including environmental chemicals, heavy metals, pesticides, and air pollutants.^{53,54} Compared with other trace elements, arsenic is abundant in the environment and presents serious complications to plants, animals, and humans via the trophic transfer through the water-soil-crop-animal-human route.⁵⁵ As a result of arsenic exposure, decreases in the productivity of edible plants lead to tremendous economic losses.⁵⁵ Regardless of the applications of arsenic treatments as a therapeutic agent for solid tumors and acute promyelocytic leukemia (APL),^{56,57} the clinical symptoms and pathophysiological findings of arsenic exposure-mediated nephrotoxicity have been described.⁵⁸ The occupational arsenic exposures in industrial workers triggered large-scale toxicity and clinical nephrotoxicity symptoms including hemolysis and acute renal failures. For centuries, numerous epidemiological and animal model studies have confirmed the potential associations between arsenic contaminations and nephrotoxicity,^{23,59} consistent with our finding about the renal dysfunctions manifested by the elevated plasma levels of BUN and CRE and histopathological alternations in the NaAsO₂ exposed mice renal tissues. Given that millions of people are potentially exposed to overdosed levels of arsenic, the positive associations between overdosed arsenic exposure in daily life and hazardous health outcomes make arsenic exposure-mediated nephrotoxicity a challenge to the global health problem.

While detailed studies examining the mechanisms related to arsenic exposure-mediated nephrotoxicity are desperately needed, emphasis is also required on identifying alternative interventions and more functional nutrients to combat or at least minimize arsenic exposure-mediated nephrotoxicity. The supplementations of proactive nutrients, including resveratrol,⁶⁰ naringenin,¹⁹ mushroom lectin,⁶¹ green tea extract,⁶² taurine,⁶³ and flaxseed oil,⁶⁴ have been considered cost-effective alternatives to ameliorate arsenic exposure-mediated nephrotoxicity. To date and to the best of our knowledge, the efficacy of SeNPs supplementations to counteract arsenic exposure-mediated nephrotoxicity or other injurious impacts has not been investigated.

According to previous publications, the size similarity between NPs and biomolecules, such as proteins and polynuclear acids, promoted the extensive applications of NPs in biology and clinical medicine.^{31,65} Due to the physiochemical characteristics including excellent bioavailability, lower toxicity, and advanced therapeutic properties compared to those of Se ions, SeNPs with high selenium loading potentials, overwhelms the low therapeutic index of organic and inorganic forms of selenocompounds.^{66,67} Meanwhile, SeNPs have been recognized as a promising tool for adjunctive therapies and preclinical researches in drug delivery, diabetes, infections, neurological diseases, nano-biosensor, and cancer prevention.^{68,69} In addition, converging lines of evidence have proved the multiple pharmacological properties and favorable therapeutic significances of SeNPs in attenuating renal injuries induced by ischemia/reperfusion, diabetes, irradiation, and exposure to drugs and nephrotoxic molecules (such as cisplatin, acetaminophen, glycerol, gentamicin, streptozotocin, melamine, and nicotine).^{27,30,34,35,70} In support of these previous reports, the present study provided fundamental evidence that the SeNPs exhibited considerable protective activity against the NaAsO₂-induced renal dysfunctions.

Prompted by the promising developments in nanotechnology, decades of research related to nanomedicine have dramatically expanded our understanding of the positive connections between the synthetic conditions of NPs and their structural, optical, and electronic properties, which in turn regulate the functions and biosafety of NPs.⁷¹ For the development of feasible, safer, inexpensive, large-scale, and environmentally friendly processes for manufacturing of SeNPs,⁷¹ the trend of SeNPs-related research is now directed towards the different fabrication systems of SeNPs via physical, chemical, and biological methods using fungi, bacteria, and plant extract as substrates, causing great scientific acclaim in the field of biomedical application of SeNPs.³⁷ In this study, SeNPs were synthesized at room temperature

with well-known chemical methods involving Na_2SeO_3 as the precursor. Moreover, glucose was added as a nontoxic stabilizer for the chemical synthesis of SeNPs to avoid the criticized conclusions due to the applications of toxic reagents in the chemical synthesis of SeNPs.^{72,73} Based on these former studies, the nontoxic reducing features of glucose supplementation benefit the chemical synthesis process of SeNPs and prevent the aggregations of SeNPs, which could be qualified as green chemical synthesis of SeNPs.^{73,74} The results of plasma parameters (BUN, CRE, ALT, AST, IL-1 β , and IL-10) between the SeNPs and NC groups demonstrated the excellent biocompatibility and safe nature of SeNPs prepared in this study. Nevertheless, the beneficial effect of glucose supplementation on the bioactivity, biocompatibility, and bioavailability of SeNPs needs more detailed investigations.

Due to the heterogeneity of nephrotoxicity, the exact pathogenesis mechanism related to the protective effects of SeNPs against NaAsO_2 exposure-mediated nephrotoxicity remains to be further investigated. However, a bundle of shreds of evidence suggests that fibrosis, inflammation, oxidative stress-related damage, and apoptosis are identified mechanisms during the pathogenesis of arsenic-mediated nephrotoxicity.^{23,75,76} In line with these findings, the nephro-protective effects of SeNPs against NaAsO_2 -mediated nephrotoxicity were analyzed by the comprehensive assessments of fibrosis, inflammation, oxidative stress-related damage, and apoptosis in mice renal tissues and HK2 cells. Expectedly, based on the in vivo and in vitro results, we found that the functionalized SeNPs supplementations not only inhibited the expression levels of fibrosis-related proteins (α -SMA and fibronectin), pro-inflammatory cytokine (IL-1 β), pro-apoptotic protein (Bax), and DNA damage related protein (γ H2A) but also up-regulated the expression levels of anti-inflammatory cytokine (IL-10) and anti-apoptotic protein (Bcl-2). Combined with the activities of antioxidant enzymes and expression patterns of oxidative stress related markers, the above results confirmed the protective effects of SeNPs against NaAsO_2 -mediated nephrotoxicity via its anti-fibrosis, anti-inflammation, antioxidant, and anti-apoptosis activities.

Despite the above experimental evidence for the protective capacity of SeNPs against NaAsO_2 -mediated nephrotoxicity, the exact causal factors responsible for the ameliorative effects of SeNPs against NaAsO_2 -mediated nephrotoxicity are not fully clear. According to these publications, a complex combination of mechanisms may be involved in the NaAsO_2 -induced toxicity ranging from cytotoxicity, DNA fragmentation, chromatin damage, disruption of antioxidant potentials, lipid peroxidation, genomic instability, suppressed immunomodulation, and altered apoptosis,^{77–79} which were partly consistent with the results obtained in the present study. In contrast, accumulating evidence have illustrated that the antioxidant SeNPs appears to be more effective than that of other Se compounds such as sodium selenite, selenomethionine, selenium methylselenocysteine, and sodium selenosulfate at inducing the biosynthesis of selenoenzymes (such as glutathione peroxidases and thioredoxin reductases) and selenoproteins.⁸⁰ Beginning with the discovery of GPx as the first mammalian selenoprotein in 1973, considerable achievements have been made in the past decades for elucidating the physiological roles of selenoenzymes or selenoproteins in the regulation of mammalian antioxidant defense systems by reducing tyrosyl radicals in proteins, degrading lipid hydroperoxides, scavenging free radicals, and preventing oxidative DNA damages and cell apoptosis.^{80,81} These former literatures have also confirmed that these characterized selenoenzymes or selenoproteins induced by SeNPs effectively diminish the outcomes of disrupted inflammatory response cascades such as the increased expression of chemoattractant cytokines, adhesive molecules, fibrogenesis, collagens, and metalloproteinase by inhibiting the activation of nuclear factor- κ B (NF- κ B) or phosphorylation of NF- κ B via redox related signaling pathways or macrophage signaling transduction pathways.^{82,83} It is also of interest that the dramatic reductions in the inflammatory response cascades decompose the proliferation of fibroblasts and then benefit the anti-fibrosis, anti-inflammatory, and antioxidant properties of SeNPs.⁸² Therefore, we speculated that the counteract capacity of SeNPs against NaAsO_2 -mediated nephrotoxicity may be related to the effective induction of antioxidant defense systems by inducing the selenoenzymes or selenoproteins, partly confirmed by the ameliorated *Gpx* expression levels in the NaAsO_2 exposed mice renal tissues after the SeNPs treatments. However, more detailed investigations remain urgently awaited to elucidate these variable and complex mechanisms.

Of particular significance, we also found that the NaAsO_2 exposure triggered the mitochondria dysfunctions in HK2 cells, partly consistent with the results of our former study.⁸ Mitochondria dysfunctions mediated nephrotoxicity has been heavily studied over past decades but continues to produce new and exciting findings.⁸⁴ Under pathological disorders, mitochondria dysfunctions triggered the damaged integrity of mitochondrial membrane potential (MMP), in turn, potentiating the release of a variety of mitochondrial components from the impaired mitochondrial into the cytoplasm

or extracellular environment and promoting downstream oxidative stress, fibrosis, and inflammatory response cascades.^{85,86} Moreover, the endonucleases from the mitochondria due to the hyperpermeable mitochondrial membranes translocate to the nuclei and cause DNA fragmentation.^{33,87} The releases of proapoptotic factors from the impaired mitochondrial also trigger nephrotoxicity by promoting apoptosis, necrosis, or autophagy.

Due to the vital functions of mitochondria in mammalian renal development, these mitochondria-related therapeutic components including elamipretide, CoQ10, and MitoQ have been used in preclinical trials through enhancing the mitochondrial functions or dampening the consequences of mitochondrial dysfunctions, including hyperpermeable mitochondrial membranes, altered mitochondrial dynamics, oxidative stress, fibrosis, overexpression of cytokines, and apoptosis.⁸⁸ Recent studies related to nanotechnology have also focused on new approaches to either preserve mitochondrial functions or promote mitochondrial biogenesis to ameliorate nephrotoxicity induced by cisplatin exposure.^{84,89} Our previous study has confirmed that Se supplementation in the form of nanomaterials effectively promoted mammalian mitochondrial functions.⁹⁰ In the present study, we also found that the mitochondria dysfunctions and the subsequent nephrotoxicity consequences of mitochondrial dysfunctions in the NaAsO₂ exposed mice renal tissues and HK2 cells were effectively ameliorated by the SeNPs supplementation. Nevertheless, the detailed signaling pathways remain to be further investigated.

Conclusion

Taken together, the above findings in the present study authentically confirmed the biosafety and nephroprotective effects of SeNPs treatments against the NaAsO₂ exposure-induced fibrosis via alleviating inflammation, oxidative stress-related damage, and apoptosis. And we hope that the nephroprotective effects of SeNPs treatments will benefit drug investigations based on the special characteristic of SeNPs and this future research related to the clinical applications of SeNPs.

Abbreviations

Na₂SeO₃, Sodium selenite; NaAsO₂, Sodium arsenite; WHO, World Health Organization; IARC, International Agency of Research on Cancer; ROS, Reactive oxygen species; MPT, Mitochondrial permeability transition; CVD, Cardiovascular disease; ER, Endoplasmic reticulum; ECM, Extracellular matrix; MMPs, Matrix metalloproteinases; TIMPs, Tissue inhibitors of metalloproteinases; Se, Selenium; NPs, Nanoparticles; SEM, Scanning electron microscopy; EDAX, Energy dispersive analysis of X-ray spectroscopy; NC, Negative control; ALT, Alanine aminotransferase; AST, Aspartate aminotransferase; BUN, Blood urea nitrogen; CRE, Creatinine; ELISA, Enzyme-linked immunosorbent assay; PBS, Phosphate buffer saline; HE, Hematoxylin & eosin staining; IHC, Immunohistochemistry; STR, Short tandem repeat; DMEM, Dulbecco's modified eagle medium; FBS, Fetal bovine serum; P/S, Penicillin/streptomycin; IF, Immunofluorescence; BSA, Bovine albumin; $\Delta\Psi_m$, Mitochondrial Membrane Potentials; PFA, Paraformaldehyde; DCFH-DA, Dichlorofluorescein diacetate; DPBS, Dulbecco's phosphate-buffered saline solution; SPSS, Statistical Package for the Social Sciences; SD, Standard deviation; APL, Acute promyelocytic leukemia; NF- κ B, Nuclear factor- κ B; DMSO, Dimethyl sulfoxide.

Data Sharing Statement

We declared that materials described in the manuscript, including all relevant raw data, will be freely available to any scientist wishing to use them for non-commercial purposes, without breaching participant confidentiality.

Ethics Approval

The permission for this study was granted by the ethics committee of Inner Mongolia Medical University (NMGYKDX-20095083-2023-M1).

Acknowledgments

We would like to express our gratitude to the staff from the animal experimental room in the College of Life Science, Inner Mongolia University for their kind help.

Funding

This work was supported by the Natural Science Foundation of Inner Mongolia (2021MS08105 to Zhenli Wu and 2021BS08028 to Shubin Li), the Joint Fund Research Project of Inner Mongolia Medical University (YKD2021LH045 to Zhenli Wu), and Internal Projects of Inner Mongolia People's Hospital (2021YN22 to Shubin Li).

Disclosure

The authors report no conflicts of interest in this work.

References

- De Francisco P, Martín-González A, Rodríguez-Martín D, Díaz S. Interactions with arsenic: mechanisms of toxicity and cellular resistance in eukaryotic microorganisms. *Int J Environ Res Public Health*. 2021;18(22):12226. doi:10.3390/ijerph182212226
- Cantoni O, Zito E, Guidarelli A, Fiorani M, Ghezzi P. Mitochondrial ROS, ER stress, and Nrf2 crosstalk in the regulation of mitochondrial apoptosis induced by arsenite. *Antioxidants*. 2022;11(5):1034. doi:10.3390/antiox11051034
- Hughes MF. Arsenic toxicity and potential mechanisms of action. *Toxicol Lett*. 2002;133(1):1–16. doi:10.1016/s0378-4274(02)00084-x
- Mawia AM, Hui S, Zhou L, et al. Inorganic arsenic toxicity and alleviation strategies in rice. *J Hazard Mater*. 2021;408:124751. doi:10.1016/j.jhazmat.2020.124751
- Zhao J, Li A, Mei Y, et al. The association of arsenic exposure with hypertension and blood pressure: a systematic review and dose-response meta-analysis. *Environ Pollut*. 2021;289:117914. doi:10.1016/j.envpol.2021.117914
- Danes JM, Palma FR, Bonini MG. Arsenic and other metals as phenotype driving electrophiles in carcinogenesis. *Semin Cancer Biol*. 2021;76:287–291. doi:10.1016/j.semcancer.2021.09.012
- Chen QY, Costa M. Arsenic: a global environmental challenge. *Annu Rev Pharmacol Toxicol*. 2021;61:47–63. doi:10.1146/annurev-pharmtox-030220-013418
- Ren J, Li S, Wang C, et al. Glutathione protects against the meiotic defects of ovine oocytes induced by arsenic exposure via the inhibition of mitochondrial dysfunctions. *Ecotoxicol Environ Saf*. 2021;230:113135. doi:10.1016/j.ecoenv.2021.113135
- Khanam R, Kumar I, Oladapo-Shittu O, et al. Prenatal environmental metal exposure and preterm birth: a scoping review. *Int J Environ Res Public Health*. 2021;18(2):573. doi:10.3390/ijerph18020573
- Renu K, Madhyastha H, Madhyastha R, Maruyama M, Vinayagam S, Valsala Gopalakrishnan A. Review on molecular and biochemical insights of arsenic-mediated male reproductive toxicity. *Life Sci*. 2018;212:37–58. doi:10.1016/j.lfs.2018.09.045
- Smeester L, Rager JE, Bailey KA, et al. Epigenetic changes in individuals with arsenicosis. *Chem Res Toxicol*. 2011;24(2):165–167. doi:10.1021/tx1004419
- Nava-Rivera LE, Betancourt-Martínez ND, Lozoya-Martínez R, et al. Transgenerational effects in DNA methylation, genotoxicity and reproductive phenotype by chronic arsenic exposure. *Sci Rep*. 2021;11(1):8276. doi:10.1038/s41598-021-87677-y
- Kumar Sharma A, Kaur A, Kaur T, Kaur S, Pathak D, Singh AP. Ameliorative role of inducible nitric oxide synthase inhibitors against sodium arsenite-induced renal and hepatic dysfunction in rats. *Drug Chem Toxicol*. 2021;1–7. doi:10.1080/01480545.2021.1926109
- Sharma AK, Kaur J, Kaur T, et al. Ameliorative role of bosentan, an endothelin receptor antagonist, against sodium arsenite-induced renal dysfunction in rats. *Environ Sci Pollut Res Int*. 2021;28(6):7180–7190. doi:10.1007/s11356-020-11035-0
- Sharma S, Kaur T, Sharma AK, et al. Betaine attenuates sodium arsenite-induced renal dysfunction in rats. *Drug Chem Toxicol*. 2021;1–8. doi:10.1080/01480545.2021.1959699
- Gonzalez-Cortes T, Recio-Vega R, Lantz RC, Chau BT. DNA methylation of extracellular matrix remodeling genes in children exposed to arsenic. *Toxicol Appl Pharmacol*. 2017;329:140–147. doi:10.1016/j.taap.2017.06.001
- Armutcu F, Demircan K, Yildirim U, Namuslu M, Yagmurca M, Celik HT. Hypoxia causes important changes of extracellular matrix biomarkers and ADAMTS proteinases in the Adriamycin-induced renal fibrosis model. *Nephrology*. 2019;24(8):863–875. doi:10.1111/nep.13572
- Campanholle G, Ligresti G, Gharib SA, Duffield JS. Cellular mechanisms of tissue fibrosis. 3. Novel mechanisms of kidney fibrosis. *Am J Physiol Cell Physiol*. 2013;304(7):C591–603. doi:10.1152/ajpcell.00414.2012
- Mershiba SD, Dassprakash MV, Saraswathy SD. Protective effect of naringenin on hepatic and renal dysfunction and oxidative stress in arsenic intoxicated rats. *Mol Biol Rep*. 2013;40(5):3681–3691. doi:10.1007/s11033-012-2444-8
- Jalaludeen AM, Lee WY, Kim JH, et al. Therapeutic efficacy of biochanin A against arsenic-induced renal and cardiac damage in rats. *Environ Toxicol Pharmacol*. 2015;39(3):1221–1231. doi:10.1016/j.etap.2015.04.020
- Gonca S, Ceylan S, Yardimoğlu M, et al. Protective effects of vitamin E and selenium on the renal morphology in rats fed high-cholesterol diets. *Pathobiology*. 2000;68(6):258–263. doi:10.1159/000055935
- Gong X, Ivanov VN, Davidson MM, Hei TK. Tetramethylpyrazine (TMP) protects against sodium arsenite-induced nephrotoxicity by suppressing ROS production, mitochondrial dysfunction, pro-inflammatory signaling pathways and programmed cell death. *Arch Toxicol*. 2015;89(7):1057–1070. doi:10.1007/s00204-014-1302-y
- Al-Megrin WA, Metwally DM, Habotta OA, Amin HK, Abdel Moneim AE, El-Khadragy M. Nephroprotective effects of chlorogenic acid against sodium arsenite-induced oxidative stress, inflammation, and apoptosis. *J Sci Food Agric*. 2020;100(14):5162–5170. doi:10.1002/jsfa.10565
- Zheng Z, Deng G, Qi C, et al. Porous Se@SiO₂ nanospheres attenuate ischemia/reperfusion (I/R)-induced acute kidney injury (AKI) and inflammation by antioxidative stress. *Int J Nanomedicine*. 2019;14:215–229. doi:10.2147/ijn.s184804
- Wang S, Chen Y, Han S, et al. Selenium nanoparticles alleviate ischemia reperfusion injury-induced acute kidney injury by modulating GPx-1/NLRP3/Caspase-1 pathway. *Theranostics*. 2022;12(8):3882–3895. doi:10.7150/thno.70830
- Khater SI, Mohamed AA, Arisha AH, et al. Stabilized-chitosan selenium nanoparticles efficiently reduce renal tissue injury and regulate the expression pattern of aldose reductase in the diabetic-nephropathy rat model. *Life Sci*. 2021;279:119674. doi:10.1016/j.lfs.2021.119674

27. Zheng S, Hameed Sultan A, Kurtas PT, Kareem LA, Akbari A. Comparison of the effect of vitamin C and selenium nanoparticles on gentamicin-induced renal impairment in male rats: a biochemical, molecular and histological study. *Toxicol Mech Methods*. 2022;1–11. doi:10.1080/15376516.2022.2124136
28. Ahmed ZSO, Galal MK, Drweesh EA, et al. Protective effect of starch-stabilized selenium nanoparticles against melamine-induced hepato-renal toxicity in male albino rats. *Int J Biol Macromol*. 2021;191:792–802. doi:10.1016/j.ijbiomac.2021.09.156
29. Al-Brakati A, Alsharif KF, Alzahrani KJ, et al. Using green biosynthesized lycopene-coated selenium nanoparticles to rescue renal damage in glycerol-induced acute kidney injury in rats. *Int J Nanomedicine*. 2021;16:4335–4349. doi:10.2147/ijn.s306186
30. AlBasher G, Alfarraj S, Alarifi S, et al. Nephroprotective role of selenium nanoparticles against glycerol-induced acute kidney injury in rats. *Biol Trace Elem Res*. 2020;194(2):444–454. doi:10.1007/s12011-019-01793-5
31. Karami M, Asri-Rezaei S, Dormanesh B, Nazarizadeh A. Comparative study of radioprotective effects of selenium nanoparticles and sodium selenite in irradiation-induced nephropathy of mice model. *Int J Radiat Biol*. 2018;94(1):17–27. doi:10.1080/09553002.2018.1400709
32. Zaghloul RA, Abdelghany AM, Samra YA. Rutin and selenium nanoparticles protected against STZ-induced diabetic nephropathy in rats through downregulating Jak-2/Stat3 pathway and upregulating Nrf-2/HO-1 pathway. *Eur J Pharmacol*. 2022;933:175289. doi:10.1016/j.ejphar.2022.175289
33. Sadek KM, Lebda MA, Abouzied TK, Nasr SM, Shoukry M. Neuro- and nephrotoxicity of subchronic cadmium chloride exposure and the potential chemoprotective effects of selenium nanoparticles. *Metab Brain Dis*. 2017;32(5):1659–1673. doi:10.1007/s11011-017-0053-x
34. Abu-Zeid EH, Abdel Fattah DM, Arisha AH, et al. Protective prospects of eco-friendly synthesized selenium nanoparticles using Moringa oleifera or Moringa oleifera leaf extract against melamine induced nephrotoxicity in male rats. *Ecotoxicol Environ Saf*. 2021;221:112424. doi:10.1016/j.ecoenv.2021.112424
35. Li X, Wang Q, Deng G, et al. Porous Se@SiO₂ nanospheres attenuate cisplatin-induced acute kidney injury via activation of Sirt1. *Toxicol Appl Pharmacol*. 2019;380:114704. doi:10.1016/j.taap.2019.114704
36. Li Y, Li X, Wong YS, et al. The reversal of cisplatin-induced nephrotoxicity by selenium nanoparticles functionalized with 11-mercapto-1-undecanol by inhibition of ROS-mediated apoptosis. *Biomaterials*. 2011;32(34):9068–9076. doi:10.1016/j.biomaterials.2011.08.001
37. Zahran WE, Elsonbaty SM, Moawad FSM. Selenium nanoparticles with low-level ionizing radiation exposure ameliorate nicotine-induced inflammatory impairment in rat kidney. *Environ Sci Pollut Res Int*. 2017;24(24):19980–19989. doi:10.1007/s11356-017-9558-4
38. Li Y, Li X, Zheng W, Fan C, Zhang Y, Chen T. Functionalized selenium nanoparticles with nephroprotective activity, the important roles of ROS-mediated signaling pathways. *J Mater Chem B*. 2013;1(46):6365–6372. doi:10.1039/c3tb21168a
39. Al-Quraishy S, Dkhil MA, Abdel Moneim AE. Anti-hyperglycemic activity of selenium nanoparticles in streptozotocin-induced diabetic rats. *Int J Nanomedicine*. 2015;10:6741–6756. doi:10.2147/ijn.s91377
40. Chen H, Yoo JW, Liu Y, Zhao G. Green synthesis and characterization of se nanoparticles and nanorods. *Electron Mater Lett*. 2011;7:333–336. doi:10.1007/s13391-011-0420-4
41. Hozyen HF, Khalil HMA, Ghandour RA, Al-Mokaddem AK, Amer MS, Azouz RA. Nano selenium protects against deltamethrin-induced reproductive toxicity in male rats. *Toxicol Appl Pharmacol*. 2020;408:115274. doi:10.1016/j.taap.2020.115274
42. Liu G, Li S, Yuan H, et al. Effect of sodium alginate on mouse ovary vitrification. *Theriogenology*. 2018;113:78–84. doi:10.1016/j.theriogenology.2018.02.006
43. Liu G, Wang B, Li S, Jin Q, Dai Y. Human breast cancer decellularized scaffolds promote epithelial-to-mesenchymal transitions and stemness of breast cancer cells in vitro. *J Cell Physiol*. 2019;234(6):9447–9456. doi:10.1002/jcp.27630
44. Jin Q, Liu G, Li SB, et al. Decellularized breast matrix as bioactive microenvironment for in vitro three-dimensional cancer culture. Article. *J Cell Physiol*. 2019;234(4):3425–3435. doi:10.1002/jcp.26782
45. Chang YW, Singh KP. Arsenic induces fibrogenic changes in human kidney epithelial cells potentially through epigenetic alterations in DNA methylation. *J Cell Physiol*. 2019;234(4):4713–4725. doi:10.1002/jcp.27244
46. Li S, Liu M, Ma H, et al. Ameliorative effect of recombinant human lactoferrin on the premature ovarian failure in rats after cyclophosphamide treatments. *J Ovarian Res*. 2021;14(1):17. doi:10.1186/s13048-020-00763-z
47. Lokanadhan G, Dass R, Kalagatur N. Phytofabrication of selenium nanoparticles from emblica officinalis fruit extract and exploring its biopotential applications: antioxidant, antimicrobial, and biocompatibility. *Front Microbiol*. 2019;10:931. doi:10.3389/fmicb.2019.00931
48. Vicaş S, Vasile L, Timar A, et al. Nano selenium—enriched probiotics as functional food products against cadmium liver toxicity. *Materials*. 2021;14:2257. doi:10.3390/ma14092257
49. Mehrzadi S, Goudarzi M, Fatemi I, Basir Z, Malayeri A, Khalili H. Chrysin attenuates sodium arsenite-induced nephrotoxicity in rats by suppressing oxidative stress and inflammation. *Tissue Cell*. 2021;73:101657. doi:10.1016/j.tice.2021.101657
50. Medda N, Patra R, Ghosh TK, Maiti S. Neurotoxic mechanism of arsenic: synergistic effect of mitochondrial instability, oxidative stress, and hormonal-neurotransmitter impairment. *Biol Trace Elem Res*. 2020;198(1):8–15. doi:10.1007/s12011-020-02044-8
51. Chatterjee A, Chatterji U. All-trans retinoic acid ameliorates arsenic-induced oxidative stress and apoptosis in the rat uterus by modulating MAPK signaling proteins. *J Cell Biochem*. 2017;118(11):3796–3809. doi:10.1002/jcb.26029
52. Samelo RR, da Cunha de Medeiros P, de Carvalho Cavalcante DN, et al. Low concentrations of sodium arsenite induce hepatotoxicity in prepubertal male rats. *Environ Toxicol*. 2020;35(5):553–560. doi:10.1002/tox.22890
53. Paithankar JG, Saini S, Dwivedi S, Sharma A, Chowdhuri DK. Heavy metal associated health hazards: an interplay of oxidative stress and signal transduction. *Chemosphere*. 2021;262:128350. doi:10.1016/j.chemosphere.2020.128350
54. Rahaman MS, Rahman MM, Mise N, et al. Environmental arsenic exposure and its contribution to human diseases, toxicity mechanism and management. *Environ Pollut*. 2021;289:117940. doi:10.1016/j.envpol.2021.117940
55. Rehman MU, Khan R, Khan A, et al. Fate of arsenic in living systems: implications for sustainable and safe food chains. *J Hazard Mater*. 2021;417:126050. doi:10.1016/j.jhazmat.2021.126050
56. Luo X, Gong X, Su L, et al. Activatable mitochondria-targeting organoarsenic prodrugs for bioenergetic cancer therapy. *Angew Chem Int Ed Engl*. 2021;60(3):1403–1410. doi:10.1002/anie.202012237
57. Chen S, Wu JL, Liang Y, et al. Arsenic trioxide rescues structural p53 mutations through a cryptic allosteric site. *Cancer Cell*. 2021;39(2):225–239. e8. doi:10.1016/j.ccell.2020.11.013
58. Robles-Osorio ML, Sabath-Silva E, Sabath E. Arsenic-mediated nephrotoxicity. *Ren Fail*. 2015;37(4):542–547. doi:10.3109/0886022x.2015.1013419

59. Tian X, Xie J, Chen X, et al. Deregulation of autophagy is involved in nephrotoxicity of arsenite and fluoride exposure during gestation to puberty in rat offspring. *Arch Toxicol.* **2020**;94(3):749–760. doi:10.1007/s00204-019-02651-y
60. Yu M, Xue J, Li Y, et al. Resveratrol protects against arsenic trioxide-induced nephrotoxicity by facilitating arsenic metabolism and decreasing oxidative stress. *Arch Toxicol.* **2013**;87(6):1025–1035. doi:10.1007/s00204-013-1026-4
61. Bera AK, Rana T, Das S, et al. Mitigation of arsenic-mediated renal oxidative stress in rat by Pleurotus Florida lectin. *Hum Exp Toxicol.* **2011**;30(8):940–951. doi:10.1177/0960327110384521
62. Messarah M, Saoudi M, Boumendjel A, Kadeche L, Boulakoud MS, El Feki A. Green tea extract alleviates arsenic-induced biochemical toxicity and lipid peroxidation in rats. *Toxicol Ind Health.* **2013**;29(4):349–359. doi:10.1177/0748233711433934
63. Roy A, Manna P, Sil PC. Prophylactic role of taurine on arsenic mediated oxidative renal dysfunction via MAPKs/ NF-kappaB and mitochondria dependent pathways. *Free Radic Res.* **2009**;43(10):995–1007. doi:10.1080/10715760903164998
64. Rizwan S, Naqshbandi A, Farooqui Z, Khan AA, Khan F. Protective effect of dietary flaxseed oil on arsenic-induced nephrotoxicity and oxidative damage in rat kidney. *Food Chem Toxicol.* **2014**;68:99–107. doi:10.1016/j.fct.2014.03.011
65. De M, Ghosh PS, Rotello VM. Applications of Nanoparticles in Biology. *Adv Mater.* **2008**;20:4225–4241.
66. Ezhuthupurakkal PB, Polaki LR, Suyavaran A, Subastri A, Sujatha V, Thirunavukkarasu C. Selenium nanoparticles synthesized in aqueous extract of Allium sativum perturbs the structural integrity of Calf thymus DNA through intercalation and groove binding. *Mater Sci Eng C Mater Biol Appl.* **2017**;74:597–608. doi:10.1016/j.msec.2017.02.003
67. IARC. Some drinking-water disinfectants and contaminants, including arsenic. *IARC Monogr Eval Carcinog Risks Hum.* **2004**;84:1–477.
68. Hong A, Rao L, Zhuang M, Luo T, Wang Y, Ma Y. Chitosan-decorated selenium nanoparticles as protein carriers to improve the in vivo half-life of the peptide therapeutic BAY 55-9837 for type 2 diabetes mellitus. *Int J Nanomedicine.* **2014**;4819. doi:10.2147/IJN.S67871
69. Kumar GS, Kulkarni A, Khurana A, Kaur J, Tikoo K. Selenium nanoparticles involve HSP-70 and SIRT1 in preventing the progression of type 1 diabetic nephropathy. *Chem Biol Interact.* **2014**;223:125–133. doi:10.1016/j.cbi.2014.09.017
70. Saif-Elnasr M, Abdel-Aziz N, El-Batal AI. Ameliorative effect of selenium nanoparticles and fish oil on cisplatin and gamma irradiation-induced nephrotoxicity in male albino rats. *Drug Chem Toxicol.* **2018**;42(1):94–103. doi:10.1080/01480545.2018.1497050
71. Sarkar J, Mridha D, Davoodbasha MA, et al. A state-of-the-art systemic review on selenium nanoparticles: mechanisms and factors influencing biogenesis and its potential applications. *Biol Trace Elem Res.* **2023**. doi:10.1007/s12011-022-03549-0
72. Nie T, Wu H, Wong K-H, Chen T. Facile synthesis of highly uniform selenium nanoparticles using glucose as the reductant and surface decorator to induce cancer cell apoptosis. *J Mater Chem B.* **2016**;4(13):2351–2358. doi:10.1039/C5TB02710A
73. Sentkowska A, Pyrzyńska K. the influence of synthesis conditions on the antioxidant activity of selenium nanoparticles. *Molecules.* **2022**;27(8):2486. doi:10.3390/molecules27082486
74. Borowska M, Giersz J, Jankowski K. Analytical monitoring of selenium nanoparticles green synthesis using photochemical vapor generation coupled with MIP-OES and UV–Vis spectrophotometry. *Microchem J.* **2018**;145. doi:10.1016/j.microc.2018.12.024
75. Barnett LMA, Cummings BS. Nephrotoxicity and renal pathophysiology: a contemporary perspective. *Toxicol Sci.* **2018**;164(2):379–390. doi:10.1093/toxsci/kfy159
76. Wan F, Zhong G, Wu S, et al. Arsenic and antimony co-induced nephrotoxicity via autophagy and pyroptosis through ROS-mediated pathway in vivo and in vitro. *Ecotoxicol Environ Saf.* **2021**;221:112442. doi:10.1016/j.ecoenv.2021.112442
77. Momeni HR, Eskandari N. Effect of curcumin on kidney histopathological changes, lipid peroxidation and total antioxidant capacity of serum in sodium arsenite-treated mice. *Exp Toxicol Pathol.* **2017**;69(2):93–97. doi:10.1016/j.etp.2016.08.006
78. Riedmann C, Ma Y, Melikishvili M, et al. Inorganic Arsenic-induced cellular transformation is coupled with genome wide changes in chromatin structure, transcriptome and splicing patterns. *BMC Genomics.* **2015**;16(1):212. doi:10.1186/s12864-015-1295-9
79. Yu H, Kuang M, Wang Y, et al. Sodium arsenite injection induces ovarian oxidative stress and affects steroidogenesis in rats. *Biol Trace Elem Res.* **2019**;189(1):186–193. doi:10.1007/s12011-018-1467-y
80. Rezvanfar MA, Rezvanfar MA, Shahverdi AR, et al. Protection of cisplatin-induced spermatotoxicity, DNA damage and chromatin abnormality by selenium nano-particles. *Toxicol Appl Pharmacol.* **2013**;266(3):356–365. doi:10.1016/j.taap.2012.11.025
81. Li S, Ren J, Zhang W, et al. Glutathione and selenium nanoparticles have a synergistic protective effect during cryopreservation of bull semen. Original Research. *Front Vet Sci.* **2023**;10. doi:10.3389/fvets.2023.1093274
82. Miroliaee AE, Esmaily H, Vaziri-Bami A, Baeri M, Shahverdi AR, Abdollahi M. Amelioration of experimental colitis by a novel nanoselenium-silymarin mixture. *Toxicol Mech Methods.* **2011**;21(3):200–208. doi:10.3109/15376516.2010.547887
83. Duntas LH. Selenium and inflammation: underlying anti-inflammatory mechanisms. *Horm Metab Res.* **2009**;41(06):443–447. doi:10.1055/s-0029-1220724
84. Davoudi M, Jadidi Y, Moayedi K, Farrokhi V, Afrisham R. Ameliorative impacts of polymeric and metallic nanoparticles on cisplatin-induced nephrotoxicity: a 2011–2022 review. *J Nanobiotechnology.* **2022**;20(1):504. doi:10.1186/s12951-022-01718-w
85. Masubuchi Y, Suda C, Horie T. Involvement of mitochondrial permeability transition in Acetaminophen-induced liver injury in mice. *J Hepatol.* **2005**;42(1):110–116. doi:10.1016/j.jhep.2004.09.015
86. Jin L, Yu B, Armando I, Han F. Mitochondrial DNA-mediated inflammation in acute kidney injury and chronic kidney disease. *Oxid Med Cell Longev.* **2021**;2021:1–12. doi:10.1155/2021/9985603
87. Bajt ML, Cover C, Lemasters JJ, Jaeschke H. Nuclear translocation of endonuclease G and apoptosis-inducing factor during Acetaminophen-induced liver cell injury. *Toxicol Sci.* **2006**;94(1):217–225. doi:10.1093/toxsci/kfl077
88. Fontecha-Barriuso M, Lopez-Diaz AM, Guerrero-Mauvecin J, et al. Tubular mitochondrial dysfunction, oxidative stress, and progression of chronic kidney disease. *Antioxidants.* **2022**;11(7):1356. doi:10.3390/antiox11071356
89. Dehghani MA, Shakiba Maram N, Moghimipour E, Khorsandi L, Atefi Kah M, Mahdavinia M. Protective effect of gallic acid and gallic acid-loaded Eudragit-RS 100 nanoparticles on cisplatin-induced mitochondrial dysfunction and inflammation in rat kidney. *Biochim Biophys Acta Mol Basis Dis.* **2020**;1866(12):165911. doi:10.1016/j.bbdis.2020.165911
90. Wang M, Ren J, Liu Z, et al. Beneficial Effect of selenium doped carbon quantum dots supplementation on the in vitro development competence of ovine oocytes. *Int J Nanomedicine.* **2022**;17:2907–2924. doi:10.2147/ijn.s360000

International Journal of Nanomedicine**Dovepress****Publish your work in this journal**

The International Journal of Nanomedicine is an international, peer-reviewed journal focusing on the application of nanotechnology in diagnostics, therapeutics, and drug delivery systems throughout the biomedical field. This journal is indexed on PubMed Central, MedLine, CAS, SciSearch®, Current Contents®/Clinical Medicine, Journal Citation Reports/Science Edition, EMBase, Scopus and the Elsevier Bibliographic databases. The manuscript management system is completely online and includes a very quick and fair peer-review system, which is all easy to use. Visit <http://www.dovepress.com/testimonials.php> to read real quotes from published authors.

Submit your manuscript here: <https://www.dovepress.com/international-journal-of-nanomedicine-journal>